International Journal of Nanomedicine

Dovepress
open access to scientific and medical research

Open Access Full Text Article

ORIGINAL RESEARCH

Antioxidant and hepatoprotective role of gold nanoparticles against murine hepatic schistosomiasis

International Journal of Nanomedicine downloaded from https://www.dovepress.com/
For personal use only.

This article was published in the following Dove Press journal:
International Journal of Nanomedicine
16 December 2015
Number of times this article has been viewed

Mohamed A Dkhil[1,2]
Amira A Bauomy[2,3]
Marwa SM Diab[4]
Saleh Al-Quraishy[2]

[1]Department of Zoology, College of Science, King Saud University, Riyadh, Saudi Arabia; [2]Department of Zoology and Entomology, Faculty of Science, Helwan University, Cairo, Egypt; [3]Department of Laboratory Sciences, College of Science & Arts, Qassim University, Buraydah, Saudi Arabia; [4]Molecular Drug Evaluation Department, National Organization for Drug Control & Research (NODCAR), Giza, Egypt

Abstract: In recent years, gold nanoparticles (AuNPs) have become the focus of much attention in biomedical research, especially in the context of nanomedicine, due to their distinctive physicochemical properties. The current study was planned to assess the effect of three dose levels of AuNPs on the gene expression, histology, and oxidative stress status of *Schistosoma mansoni*-infected mice liver. Inoculation of mice with 100 µL AuNPs at different doses (0.25, 0.5, and 1 mg/kg mice body weight) twice on day 46 and day 49 postinfection reduced the total worm burden, the egg load in the liver, and the granuloma size. AuNPs also appeared to decrease the activities of malondialdehyde and nitric oxide significantly, and increase the level of glutathione compared to the infected untreated group. Concomitantly, AuNPs ameliorated the inflammatory response by decreasing the mRNA expression of interleukin-1β, interleukin-6, tumor necrosis factor-α, interferon-γ, and inducible nitric oxide synthase. These consistent molecular, histopathological, and biochemical data suggest that AuNPs could ameliorate infection-induced damage in the livers of mice. Our results indicated that AuNPs are effective anti-schistosomal and antioxidant agents. Further confirmation of the role of nanogold as an anti-schistosomal agent, as well as its mechanism of action, requires further studies to be undertaken in the future.

Keywords: nanogold, *Schistosoma mansoni*, liver, gene expressions, histopathology, oxidative stress, mice

Introduction

Bilharziasis is one of the most common parasitic diseases, mostly affecting the liver by causing the formation of granuloma and hepatic fibrosis. The disease is considered an important helminthic infection since it is associated with severe morbidity. Schistosomiasis excessively affects people who have limited access to potable water and sanitation living in the tropics and subtropics; ~240 million people are infected, with >700 million people at risk of getting infected.[1] The standard treatment for schistosomiasis is praziquantel (PZQ); while this is known to be an effective anti-schistosomal drug, reinfection occurs rapidly, even after massive drug administration, meaning that it is not an efficient therapy, especially in *Schistosoma mansoni*-endemic areas.

Chrysotherapy, the use of gold to treat diseases such as smallpox, skin ulcers, syphilis, and measles, is attested in ancient cultures in Egypt, India, and the People's Republic of China.[2] More recently, gold complexes have also showed potential antileishmanial and antimalarial activity,[3] with an interesting role against *Leishmania* promastigotes in culture media, and apparently larvicidal properties against a mosquito vector of malaria.[4,5] They are also promising for use as "band-aids" to treat skin lesions.[6]

Correspondence: Marwa SM Diab
Molecular Drug Evaluation Department, National Organization for Drug Control & Research (NODCAR), 6 Abou Hazem St., Madkour Station, Pyramids Ave, PO Box 29, Giza 12553, Egypt
Tel +2 02 3585 0005
Fax +2 02 3585 5582
Email marwa.db@gmail.com

© 2015 Dkhil et al. This work is published and licensed by Dove Medical Press Limited. The full terms of this license are available at https://www.dovepress.com/terms.php and incorporate the Creative Commons Attribution – Non Commercial (unported, v3.0) License (http://creativecommons.org/licenses/by-nc/3.0/). By accessing the work you hereby accept the Terms. Non-commercial uses of the work are permitted without any further permission from Dove Medical Press Limited, provided the work is properly attributed. For permission for commercial use of this work, please see paragraphs 4.2 and 5 of our Terms (https://www.dovepress.com/terms.php).

Additionally, in vivo investigations are being conducted to determine the antihelminthic efficacy of gold nanoparticles (AuNPs).[7] Research on the use of gold for the treatment of human tropical diseases is therefore now considerable,[8] but studies have also focused on using AuNPs in the context of diagnosis and drug delivery.[2,9,10] For example, employing AuNPs in polymerase chain reaction (PCR) has optimized the specificity of this diagnostic method.[11] Some researchers, meanwhile, have taken advantage of AuNPs as a means of transferring drugs into biological cells as a basis for nuclear-targeted delivery,[12] and they have a strong potential role in cancer treatment and apoptosis induction.[13] Accumulation of nanosystems at the targeted site is often higher than normal drugs and usually leads to reduced systemic toxicity. The present work, therefore, aims to determine the cure rate of three doses of AuNPs against hepatic injury induced by schistosomiasis in CD-1 mice.

Materials and methods

Gold nanoparticles

AuNPs were prepared by the chemical reduction method as reported by Turkevich et al.[14] A solution of $HAuCl_4$ was used as an Au^{3+} ions precursor, while sodium citrate was used as both a mild reducing and stabilizing agent. The solution slowly turned into a faint pink color, indicating the reduction of the Au^{3+} ions to AuNPs. The fabrication of AuNPs was performed through a colloidal reduction process of chloroauric acid ($HAuCl_4 \cdot 3H_2O$) with salt of trisodium citrate ($N_3C_6H_5O_7$) purchased from Aldrich Chemical Co. Ltd. (99% pure) and used without further purification. In a typical experiment, 2 mM $HAuCl_4 \cdot 3H_2O$ was dissolved in 100 mL of double distilled water. To this solution, 1% $N_3C_6H_5O_7$ (~3 mM) was mixed drop by drop via micropipette, and the pH was measured with a pH meter (Cole-Parmer, Vernon Hills, IL, USA), which was shown to reach 7.88. The obtained pinkish-colored solution was stirred vigorously and refluxed at boiling temperature for 15–20 minutes, whereupon the pinkish-colored solution changed to the deep red-colored solution typical of AuNPs. The obtained colloidal solution was analyzed for the morphological analysis via transmission electron microscopy (TEM) under 40 kHz sonication energy and stored for the further morphological and other elemental analysis.

Characterization

The size and morphology of AuNPs were characterized by using a transmission electron microscope equipped for high-resolution transmission electron microscopy (HR-TEM). Samples for HR-TEM were prepared using the colloidal solution of nanoparticles. The colloidal sample solution was sonicated for 10 minutes in a bath sonicator (40 kHz, 135 W; Cole-Parmer) for 10 minutes before the observation, dipped in a carbon-coated copper grid (400 mesh), and dried at room temperature for the morphological analysis. An HR-TEM picture was taken using a JOEL JEM 2000 EX 200 microscope at 200 kV.

Animals

Sixty male CD-1 mice weighing 18–20 g were used in all experiments. The animals were obtained from a closed random-bred colony at the Schistosome Biological Supply Center at the Theodor Bilharz Research Institute, Giza, Egypt. Animals were housed in polycarbonate boxes with steel-wire tops (not more than six animals per cage) and bedded with wood shavings. The ambient temperature was controlled at 22°C±3°C with a relative humidity of 50%±15% and a 12-hour light/dark photoperiod. Food and water were provided ad libitum. This study was approved by and conducted in accordance with the legal and ethical guidelines of the Medical Ethics Committee of the Theodor Bilharz Research Institute, Giza, Egypt (Approval No 4018/2011).

Mice infection

S. mansoni cercariae (Egyptian strain) were obtained from infected intermediate host snails (*Biomphalaria alexandrina*) and maintained at the Schistosome Biological Supply Center. Mice were infected subcutaneously with freshly shed 100±10 cercariae/mouse according to the method of Liang et al.[15]

Experimental design

The experimental animals were divided into six groups of ten mice each. Group I served as a control (noninfected); the animals in this group received saline (100 µL saline water/mouse) by intraperitoneal injection for 10 days. Groups II, III, IV, V, and VI were infected with 100±10 *S. mansoni* cercariae. The animals of groups III, IV, and V were intraperitonially inoculated with 100 µL AuNPs at different doses (0.25, 0.5, and 1 mg/kg mice body weight) twice on day 46 and day 49 postinfection, respectively. Finally, infected animals of group VI were orally administered 100 µL of PZQ (600 mg/kg mice body weight) on day 46 postinfection at an interval of 24 hours for 2 days.[16]

Study of parasitological criteria

Immediately after the mice were killed by cervical decapitation, hepatic and portomesenteric vessels were perfused in order

to recover, and subsequently count, any worms present.[17] After perfusion, a piece of liver was used to determine the number of ova in the liver, and the percentage change in egg density was determined. The percentage of eggs at various developmental stages was examined in three samples from each mouse, and the mean number of eggs at each stage/animal was determined.[18]

Sample preparation

For each group, after dissection, the livers were immediately removed from the animals and divided into three parts: the first part for RNA extraction, the second one for histopathological studies, while the third was homogenized (10%, w/v) in an ice-cold 0.1 M Tris–HCl buffer (pH 7.4). The homogenate was centrifuged at 2,000× *g* for 15 minutes at 4°C, and the resultant supernatant was used for biochemical analysis.

Histopathological investigations and granuloma size

Tissue samples of the liver of each group were immediately fixed after animal dissection in 10% neutral buffered formalin, dehydrated, and processed for paraffin sectioning. Sections were then deparaffinized and stained with hematoxylin and eosin. To assess the size of tissue granuloma, the mean diameter (μm) was measured. For each group, 30 granulomas were chosen from different hematoxylin–eosin-stained liver sections from different mice.

Assessment of oxidative stress markers

Estimation of the reduced glutathione level

The reduced glutathione (GSH) level in the liver homogenates was determined following the method of Ellman,[19] based on the reduction of Ellman's reagent with GSH to produce a yellow compound. The reduced chromogen is directly proportional to the GSH concentration, and its absorbance can be measured at 405 nm.

Determination of thiobarbituric acid-reactive substances

Thiobarbituric acid-reactive substances (TBARS) were assayed through colorimetric tests of the liver homogenates according to the method of Ohkawa et al.[20] In this method, TBARS were determined by using 1 mL of 10% trichloroacetic acid and 1 mL of 0.67% thiobarbituric acid which were then heated together in a boiling water bath for 30 minutes. TBARS, which react with the amount of malondialdehyde (MDA) found in the liver homogenate to give a red color, were then measured at 535 nm.

Determination of nitric oxide level

The nitric oxide (NO) level was assayed colorimetrically in liver homogenate according to the method of Green et al.[21] The nitrite/nitrate level was determined since, in an acid medium, and in the presence of nitrite, the formed nitrous acid-diazotized sulfanilamide is coupled with *N*-(1-naphthyl) ethylenediamine. The resulting azo dye has a bright reddish-purple color which can be measured at 540 nm.

Quantitative PCR

Tissues frozen at –80°C were thoroughly ground with a mortar under liquid nitrogen, and total RNA was isolated with Trizol (Sigma-Aldrich Co., St Louis, MO, USA). The quality and integrity of RNA were determined using the Agilent RNA 6000 Nano Kit on the Agilent 2100 Bioanalyzer (Agilent Technologies, Santa Clara, CA, USA). RNA was quantified by measuring $A_{260\ nm}$ on the ND-1000 Spectrophotometer (NanoDrop Technologies, Wilmington, DE, USA).[22] Real-time PCR was performed as detailed previously.[23,24] In brief, total RNA, freed from DNA using the DNA free kit (Applied Biosystems, Foster City, CA, USA), was used to synthesize cDNA with a Quanti Tect™ Reverse Transcription kit (Qiagen, Hilden, Germany). A Quanti Tect™ SYBR® Green PCR kit, also from Qiagen, was applied for amplifications in the ABI Prism® 7500HT Sequence Detection System (Applied Biosystems) with gene-specific Quanti Tect™ primers delivered by Qiagen. We investigated the genes encoding the mRNAs for the following proteins: interleukin (IL)-1β, tumor necrosis factor-α (TNF-α), interferon-γ (IFN-γ), and inducible nitric oxide synthase (iNOS). PCRs were performed and evaluated as detailed elsewhere.[22]

Statistical analysis

The obtained data were presented as mean ± standard error. One-way analysis of variance was carried out, and the statistical comparisons among the groups were performed with Duncan's test using a statistical package program (SPSS version 17.0). $P \leq 0.05$ was considered as significant for all statistical analyses in this study.

Results

The structural morphology and crystalline character of AuNPs were examined with a transmission electron microscope equipped for HR-TEM. The lower resolution TEM image, shown in Figure 1A, shows that AuNPs are spherical in shape and within the range of 10–15 nm in diameter. It is apparent that all the nanoparticles are in a definite spherical shape with a rough surface and are free from agglomeration behavior. The HR-TEM image of AuNPs (Figure 1B) shows

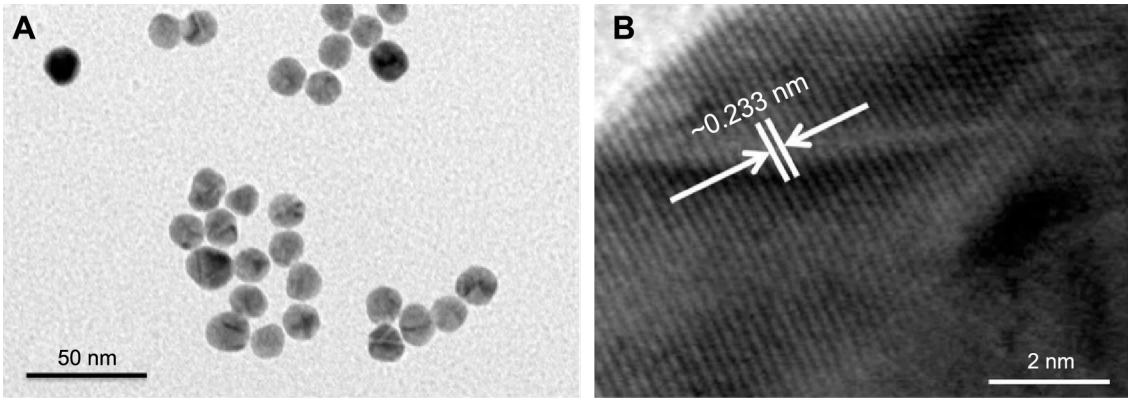

Figure 1 Typical TEM and corresponding HR-TEM images of synthesized AuNPs.
Notes: (**A**) A low-magnification image of spherical AuNPs (~10–15 nm). (**B**) An HR-TEM image of the difference between two lattice fringes, which is ~0.233 nm.
Abbreviations: TEM, transmission electron microscopy; HR-TEM, high-resolution transmission electron microscopy; AuNPs, gold nanoparticles.

that the lattice difference fringes between two adjacent planes are ~0.233 nm. The obtained lattice difference clearly corresponds to the lattice constant of face-centered cubic AuNPs and is analogous with previously reported information.[25,26] The crystal lattice fringes evident in HR-TEM (Figure 1B) confirm the good crystalline nature of synthesized AuNPs and are consistent with lower resolution images of AuNPs.[25,26] AuNPs treatment induced a significant reduction in hepatic worm burden at all examined doses (0.25, 0.5, and 1 mg/kg) compared to the infected group. The reduction in the worm burden was ~32%, 49%, and 64%, respectively (Table 1). Similarly, Figure 2 shows that the three dose levels of AuNPs caused a highly significant reduction in egg density in the liver tissues of infected mice, with the highest reduction (69.8%) being recorded for a 1 mg dose of AuNPs.

Table 2 and Figure 3 show the alternations in the liver histology between *S. mansoni*-infected animals and the control animals. Figure 3A displays a histological section of liver from a control mouse. It is apparent that the center-lobe vein has normal morphological characteristics compared to Figure 3B, which was taken from a histological section of liver after 56 days of *S. mansoni* infection. In the latter, cellular alteration is clearly apparent, with leukocyte aggregations near blood vessels and evident vascular congestion. Histological investigation of hepatic tissue sections revealed that *S. mansoni* infection caused a severe inflammatory response of the liver, as indicated by inflammatory cellular infiltration as well as cytoplasmic vacuolation and degeneration of hepatocytes. In addition, the hepatic sinusoids were dilated and apparently contained more Kupffer cells.

Table 1 Effect of gold and PZQ treatment on worms burden and egg count of schistosome infected mice

Group	Worm recovery				Reduction rate (%)
	Male	Female	Coupled	Total	
Infected	5±1	6.3±1.5	4.3±1.1	15.6±1.2	–
Infected (+0.25 mg/kg AuNPs)	4.6±1.1	5.6±1.1	0.3±0.1[a]	10.5±0.9[a]	32.7[a]
Infected (+0.5 mg/kg AuNPs)	4.3±0.9	3.3±0.6[a,b]	0.3±0.1[a]	7.9±0.7[a,b]	49.3[a,b]
Infected (+1 mg/kg AuNPs)	3±2[a,b]	2±1[a,b]	0.6±0.2[a,b]	5.6±1.2[a,b]	64.1[a,b]
Infected (+PZQ)	2.6±0.6[a,b]	1.5±0.4[a,b]	0.4±0.1[a]	4.5±0.4[a,b]	71.2[a,b]

Notes: Values are mean ± SEM. [a]Significant against non-infected (AuNPs) group at $P \leq 0.05$. [b]Significant against infected (AuNPs) group at $P \leq 0.05$.
Abbreviations: AuNPs, gold nanoparticles; SEM, standard error of the mean; PZQ, praziquantel.

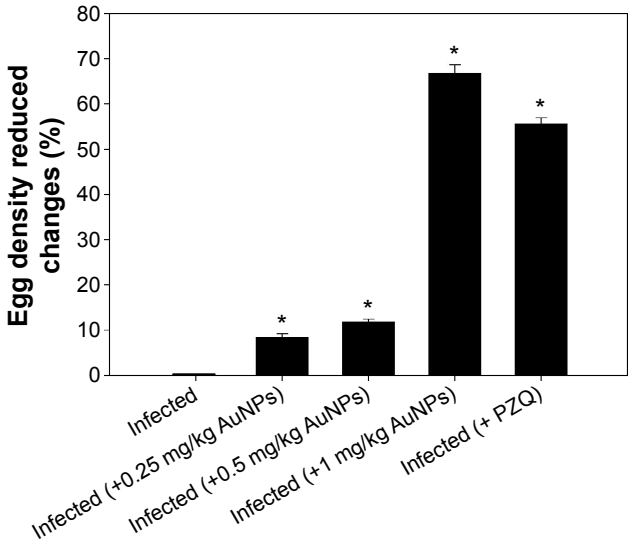

Figure 2 Egg density-induced changes in the livers of mice infected with *Schistosoma mansoni* and treated with AuNPs.
Notes: Values are mean ± SD (n=8). *Significant change at $P \leq 0.05$.
Abbreviations: AuNPs, gold nanoparticles; SD, standard deviation; PZQ, praziquantel.

Table 2 AuNPs induced alterations in the hepatic tissue of mice infected with *Schistosoma mansoni*

Group	Microscopic observation					
	Histological activity index[a]	Necrosis or apoptosis	Hemorrhage	Disorganized sinusoids	Infiltration of lymphocytes	Hyperplasia of Kupffer cells
Noninfected	2	0	0	0	0	0
Infected	14–16	+++	+++	++	+++	+++
Infected (+0.25 mg/kg AuNPs)	9–12	++	++	+	++	++
Infected (+0.5 mg/kg AuNPs)	9–11	++	++	+	++	++
Infected (+1 mg/kg AuNPs)	9–11	++	++	+	++	++
Infected (+ PZQ)	9–11	++	++	+	+++	+++

Notes: [a]According to modified Ishak et al's index.[45] Score: 1–3, minimal; 4–8, mild; 9–12, moderate; 13–18, severe. 0: absent; +: mild; ++: moderate; and +++: severe.
Abbreviations: AuNPs, gold nanoparticles; PZQ, praziquantel.

Treated livers of *S. mansoni*-infected mice at the three dose levels (0.25, 0.5, and 1 mg/kg) of AuNPs, as shown in Figure 3C–E, respectively, showed that the inflammatory cellular infiltration was moderated.

Figure 4 shows the granuloma size in hepatic tissue, with a significant reduction in the granuloma diameter apparent as a result of the treatment of schistosome-infected mice with AuNPs at all investigated doses (0.25, 0.5, and 1 mg/kg) compared to untreated infected mice ($P<0.05$). Likewise, gavaging the mice with PZQ induced a significant decrease in the hepatic granuloma size in mice infected with *S. mansoni* compared to those in the infected untreated group.

Schistosomiasis induced a significant elevation in hepatic levels of MDA and NO (Table 3). In the same manner, injection of three different doses of AuNPs and PZQ to infected mice increased the levels of MDA and NO significantly as compared to noninfected group. A significant reduction was observed in hepatic MDA and NO levels as a result of treatment with AuNPs (0.25, 0.5, and 1 mg/kg) or PZQ. Finally, GSH, which is involved in the downregulation of substances formed during oxidative stress, was determined (Table 3). It was striking that GSH was significantly downregulated by *S. mansoni* infection but that this effect was largely ameliorated by AuNPs treatment.

Moreover, the *S. mansoni*-infected mice revealed a significant upregulation in mRNA of IL-1β, IL-6, TNF-α, IFN-γ, and iNOS in hepatic tissue; likewise, injection of different doses of AuNPs and PZQ induced significant upregulation

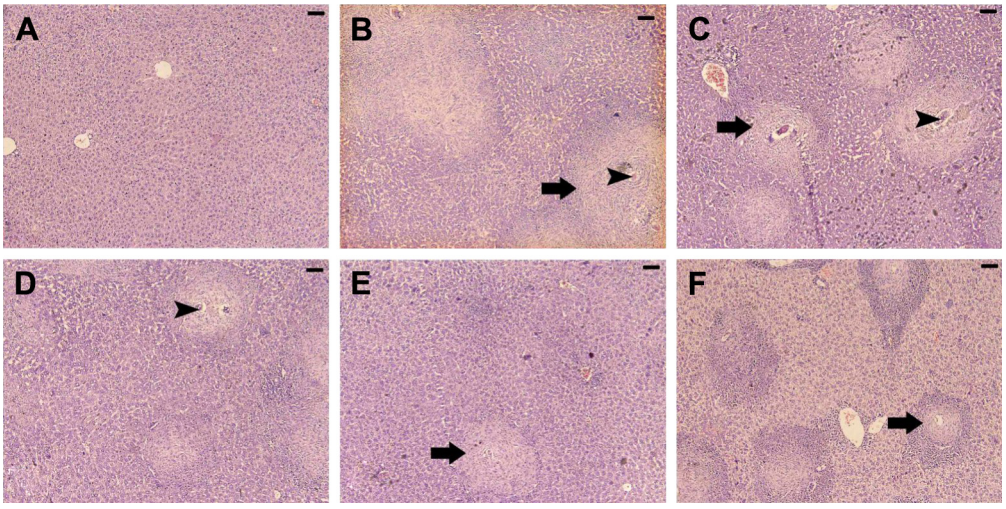

Figure 3 Histological changes in hepatic tissue of noninfected mice, untreated mice, and mice treated and infected with *Schistosoma mansoni* on day 56 postinfection.
Notes: (**A**) Noninfected liver with normal architecture. (**B**) Hepatic tissue of mice in the *S. mansoni*-infected group showing a severe inflammatory response in the liver indicated by inflammatory cellular infiltration, cytoplasmic vacuolation, degeneration of hepatocytes, dilated hepatic sinusoids dilated, and more Kupffer cells. (**C**–**E**) Hepatic tissue of mice in the *S. mansoni*-infected group treated with 0.25, 0.5, and 1 mg/kg AuNPs, respectively, showing reduced tissue damage, and (**F**) the liver of mice in the infected group treated with PZQ showing fewer lesions. Arrows indicate the inflammatory cellular infiltraion around the granuloma and arrow heads indicates enclosed eggs. Sections were stained with hematoxylin and eosin; scale bar =25 μm.
Abbreviations: AuNPs, gold nanoparticles; PZQ, praziquantel.

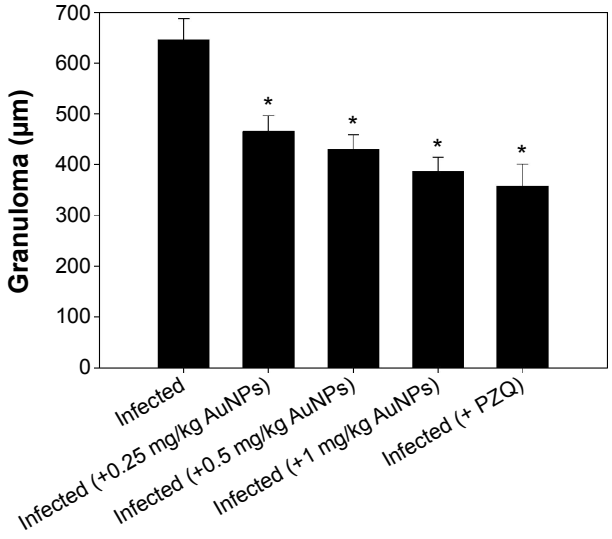

Figure 4 Reduction in granuloma size in the livers of mice infected with *Schistosoma mansoni* and treated with AuNPs.
Notes: Values are mean ± SD (n=8). *Significant change at $P \leq 0.05$.
Abbreviations: AuNPs, gold nanoparticles; SD, standard deviation; PZQ, praziquantel.

versus the control group. On the other hand, treatment with AuNPs, as with PZQ, decreased the expression of IL-1β, IL-6, TNF-α, IFN-γ, and iNOS mRNA significantly compared to the infected group (Figure 5).

Discussion

AuNPs have recently begun to be actively used for diagnostic and therapeutic applications in several fields of nanomedicine, and it has been debated that AuNPs could be used in nearly all medical purposes.[27] Abraham and Himmel[28] proved the successful usage of colloidal gold in rheumatoid arthritis patients, and AuNPs have been shown to cause cestode paralysis and death; the authors attributed this to alterations in cestode enzymatic activity of the parasite.[13]

Table 3 AuNPs induced changes in the level of hepatic GSH, MDA, and NO of mice infected with *Schistosoma mansoni*

Group	GSH (mg/kg)	MDA (nmol/g)	NO (µmol/g)
Noninfected	47.5±0.4	6±0.2	88±4
Infected	32.6±1.2[a]	44±2[a]	129±4[a]
Infected (+0.25 mg/kg AuNPs)	37.2±2[a,b]	26±1.5[a,b]	102±3.7[a,b]
Infected (+0.5 mg/kg AuNPs)	36.2±1.6[a,b]	17.5±0.7[a,b]	97±3.8[a,b]
Infected (+1 mg/kg AuNPs)	36.2±1.3[a,b]	35.2±0.2[a,b]	95±2[a,b]
Infected (+ PZQ)	35.5±1.2[a,b]	27.3±1.3[a,b]	106±2[a,b]

Notes: Values are mean ± SEM. [a]Significant against noninfected (AuNPs) group at $P \leq 0.05$. [b]Significant against infected (AuNPs) group at $P \leq 0.05$.
Abbreviations: AuNPs, gold nanoparticles; GSH, reduced glutathione; MDA, malondialdehyde; NO, nitric oxide; PZQ, praziquantel; SEM, standard error of the mean.

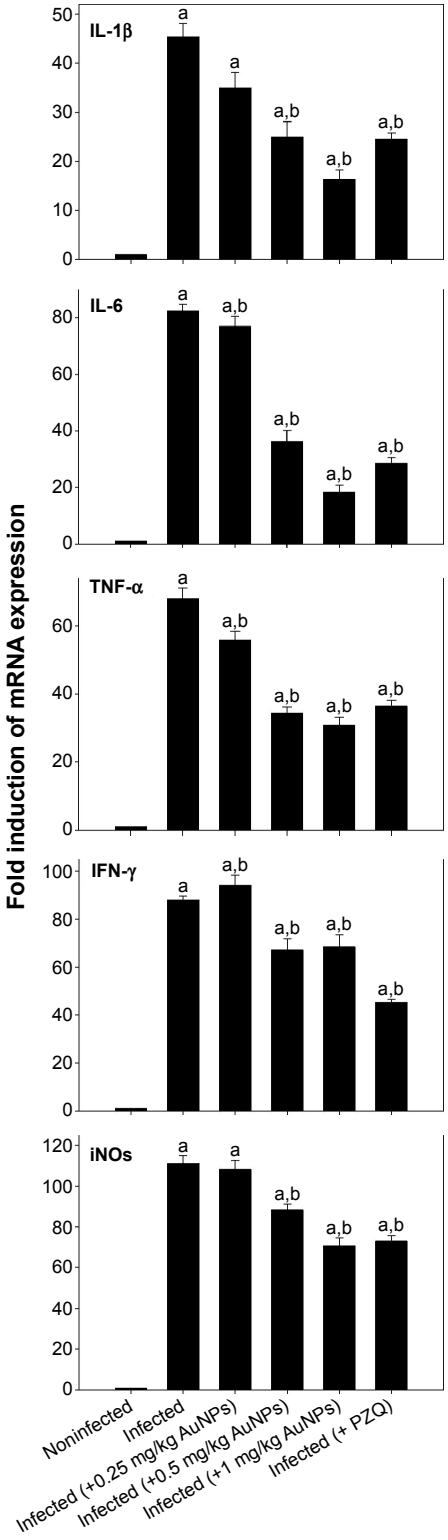

Figure 5 AuNPs induced changes in gene expression of mice livers infected with *Schistosoma mansoni*.
Notes: Expression of IL-1β, IL-6, TNF-α, IFN-γ, and iNOS in liver tissues was analyzed by quantitative RT-PCR in noninfected mice and *S. mansoni*-infected mice on day 56 postinfection with and without AuNPs treatment. Relative expression is given as fold increase in comparison with noninfected control mice. Values are mean ± SD. [a]Significant against the noninfected (AuNPs) group at $P \leq 0.05$. [b]Significant against the infected (AuNPs) group at $P \leq 0.05$.
Abbreviations: AuNPs, gold nanoparticles; IL, interleukin; TNF-α, tumor necrosis factor-α; IFN-γ, interferon-γ; iNOS, inducible nitric oxide synthase; RT-PCR, real-time polymerase chain reaction; SD, standard deviation; PZQ, praziquantel.

Our results revealed that schistosomiasis caused significant histopathological impairments in liver sections, as well as granulomatous inflammation. Amer et al[29] reported that *S. mansoni* induced granulomas as being characterized by concentric fibrosis where the trapped eggs are surrounded by many fibroblasts. In addition, Tousson et al[30] observed the main histopathological injuries in schistosomiasis as being granulomas, diffuse infiltration of inflammatory cells "eosinophils and small mononuclear cells", and fibrosis of portal areas and interlobular septa. In the same manner, El-Banhawey et al[31] stated that schistosomiasis causes necrotic changes in the liver tissues.

The treatment with different doses of AuNPs appeared to moderate inflammatory cellular infiltration, however, and to decrease the diameter of granulomas. Moreover, AuNPs reduced the hepatic worm burden compared to the infected group. This supports Dkhil et al[32] deduction that treatment of infected schistosome mice with AuNPs reduced the extent of the histological disturbances evident in the brains of infected mice.

In this study, schistosomiasis imbalanced the hepatocellular antioxidant system and liberated the free radicals, as evidenced by the decrease in GSH level and the increased levels of both nitrite/nitrate and MDA in hepatic tissue. AuNPs, however, increased hepatic GSH levels and decreased the levels of nitrite/nitrate and MDA. It has been reported that schistosomiasis disturbs the levels of enzymatic and nonenzymatic antioxidants which impairs the liver GSH content of mice and decreases the hepatic antioxidant capacity, inducing the generation of lipid peroxides which may play a main role in the pathology associated with bilharziasis.[29,33] Furthermore, *S. mansoni* is known to cause oxidative stress in different mice organs, such as brain.[34] Neuroschistosomiasis, meanwhile, also induces a reduction in GSH level and an increase in nitrite/nitrate and MDA levels, but it has been shown that injection of AuNPs (0.25, 0.5, and 1 mg/kg) into schistosome-infected mice ameliorates the GSH level and reduces levels of nitrite/nitrate and MDA in the brain tissue.[32]

In the present study, injection of AuNPs (0.25, 0.5, and 1 mg/kg) into schistosome-infected mice resulted in a significant downregulation of IL-1β, IL-6, TNF-α, IFN-γ, and iNOS mRNA expressions in hepatic tissue versus infected mice.

IL-1 and TNF-α are the major pro-inflammatory cytokines, and are considered as "alarm cytokines" which are secreted by macrophages. IL-1 plays a role in the initiation and propagation of inflammation by stimulating the expression of adhesion molecules on endothelial cells and leukocytes. In addition, TNF-α may aggravate fibrosis and reduce the granulomatous reaction due to the presence of schistosome eggs. Thus, mice lacking an IL-1β gene are characterized by delayed disease development and declined systemic inflammatory responses.[35,36] Moreover, lower expression of IL-6 and IL-1β (pro-inflammatory cytokines) causes a down-modulation of granulomatous inflammation and hepatocyte necrosis.[37] Also, macrophages could be activated to produce NO and other inflammatory mediators by IFN-γ, which is considered as an important inducer of iNOS. In addition, Abdallahi et al[38] detected iNOS mRNA in the liver at the onset of parasite egg laying; the authors showed that the levels then increased as the eggs accumulated in the liver.[39] Mwatha et al,[40] however, reported that increased TNF-γ is correlated with the development of severe hepatosplenic disease.

Khan et al[41] concluded that AuNPs (50 nm) resulted in a normal level of IL-6 gene expression in the hepatic tissue of rats on day 5 postinjection, while IL-1β and TNF-α mRNA expression was downregulated significantly on day 5. Moreover, AuNPs have no cytotoxic effect since they decrease the production of reactive oxygen species and do not stimulate secretion of pro-inflammatory cytokines (TNF-α and IL-1β) making them suitable candidates for nanomedicine.[42,43] AuNPs do not induce apoptosis, and do not activate gene expression related to oxidative stress and inflammatory response (TNF-α), while their low reactivity with biomolecules and cells provides a promising medical platform.[44,45]

Conclusion

Collectively, our investigations suggest that the way in which AuNPs exert their ameliorating effects on schistosomiasis-promoted oxidative stress may be attributed to their ability to scavenge free radicals, and that this action could find a clinical use in the treatment of hepatic dysfunction in schistosomiasis. Additional studies are still necessary, however, with a view to clarifying the exact mechanism of this modulatory effect, and to examine its potential therapeutic effects in more detail.

Acknowledgment

The authors extend their appreciation to the Deanship of Scientific Research at King Saud University for funding the work through the research group project no. RG-198.

Disclosure

The authors report no conflicts of interest in this work.

References

1. King CH. Parasites and poverty: the case of schistosomiasis. *Acta Trop*. 2010;113(2):95–104.
2. Chen PC, Mwakari SC, Oyelere AK. Gold nanoparticles: from nanomedicine to nanosensing. *Nanotechnol Sci Appl*. 2008;1:45–66.
3. Vieites M, Smircich P, Guggeri L, et al. Synthesis and characterization of a pyridine-2-thiol N-oxide gold(I) complex with potent antiproliferative effect against Trypanosoma cruzi and Leishmania sp. insight into its mechanism of action. *Inorg J Biochem*. 2009;103(10):1300–1306.
4. Navarro M, Pérez H, Sánchez-Delgado RA. Toward a novel metal-based chemotherapy against tropical diseases. 3. Synthesis and antimalarial activity in vitro and in vivo of the new gold-chloroquine complex [Au(PPh3)(CQ)]PF6. *J Med Chem*. 1997;40(12):1937–1939.
5. Navarro M, Vásquez F, Sánchez-Delgado RA, Pérez H, Sinou V, Schrével J. Toward a novel metal-based chemotherapy against tropical diseases. 7. Synthesis and in vitro antimalarial activity of new gold-chloroquine complexes. *J Med Chem*. 2004;47(21):5204–5209.
6. Balashanmugam P, Kalaichelvan PT. Biosynthesis characterization of silver nanoparticles using *Cassia roxburghii* DC. aqueous extract, and coated on cotton cloth for effective antibacterial activity. *Int J Nanomed*. 2015;10(Suppl 1):87–97.
7. Kar PK, Murmu S, Saha S, Tandon V, Acharya K. Anthelmintic efficacy of gold nanoparticles derived from a phytopathogenic fungus. *Nigrosporaoryzae*. 2014;9(1):1–9.
8. de Almeida MP, Carabineiro SAC. The role of nanogold in human tropical diseases: research, detection and therapy. *Gold Bull*. 2013;46:65–79.
9. Ghosh P, Han G, De M, Kim KC, Rotello MV. Gold nanoparticles in delivery applications. *Adv Drug Deliv Rev*. 2008;60:1307–1315.
10. Sperling RA, Gil PR, Zhang F, Zanella M, Parak WJ. Biological application of gold nanoparticles. *Chem Soc Rev*. 2008;37:1896–1908.
11. Li Z, Ji X. Association of tissue transglutaminase and NLRP3 inflammasome in liver inflammation after *Schistosoma japonicum* infection (INM6P.343). *J Immunol*. 2015;194(1 Suppl):193.17.
12. Gu YJ, Cheng J, Lin CC, Lam YW, Cheng SH, Wong WT. Nuclear penetration of surface functionalized gold nanoparticles. *Toxicol Appl Pharmacol*. 2009;237:196–204.
13. Tikhira S, Singh S, Banerjee S, Vidhyarthi AS. Biosynthesis of gold nanoparticles, scope and application: a review. *Int J Pharm Sci Res*. 2012;3(6):1603–1615.
14. Turkevich J, Stevenson PC, Hillier J. A study of the nucleation and growth processes in the synthesis of colloidal gold. *Faraday Soc*. 1951;11:55–75.
15. Liang YS, John BI, Boyd DA. Laboratory cultivation of schistosome vector snails and maintenance of schistosome life cycles. In: Proceeding of the 1st Sino-American Symposium, University of Lowell, MA, USA. Vol. 1. 1987:34–48.
16. Gonnert R, Andrews P. Praziquantel, a new broad-spectrum antischistosomal agent. *Zeitschrift fur Parasitenkunde*. 1977;52:129–150.
17. Duvall RH, De Witt WB. An improved perfusion technique for recovering adult schistosomes from laboratory animals. *Am J Trop Med Hyg*. 1967;16:483–486.
18. Pellegrino J, Oliveira CA, Faria J, Cunha AS. New approach to the screening of drugs in experimental Schistosomiasis mansoni in mice. *Am J Trop Med Hyg*. 1962;11:201–215.
19. Ellman GL. Tissue sulfhydryl groups. *Arch Biochem Biophys*. 1959;82(1):70–77.
20. Ohkawa H, Ohishi N, Yagi K. Assay for lipid peroxides in animal tissues by thiobarbituric acid reaction. *Anal Biochem*. 1979;95(2):351–358.
21. Green LC, Wagner DA, Glogowski J, Skipper PL, Wishnok JS, Tannenbaum SR. Analysis of nitrate, nitrite, and [15N] nitrate in biological fluids. *Anal Biochem*. 1982;126:131–138.
22. Delic D, Grosser C, Dkhil M, Al-Quraishy S, Wunderlich F. Testosterone-induced upregulation of miRNAs in the female mouse liver. *Steroids*. 2010;75:998–1004.
23. Dkhil MA, Abdel-Baki AS, Wunderlich F, Sies H, Al-Quraishy S. Anticoccidial and antiinflammatory activity of garlic in murine Eimeria papillata infections. *Vet Parasitol*. 2011;175(1–2):66–72.
24. Dkhil MA, Al-Quraishy S, Aref AM, Othman MS, El-Deib KM, Abdel Moneim AE. The potential role of *Azadirachta indica* treatment on cisplatin-induced hepatotoxicity and oxidative stress in female rats. *Oxid Med Cell Longev*. 2013;2013:1–9.
25. Balmes O, Malm J, Pettersson N, Karlsson G, Bovin J. Imaging atomic structure in metal nanoparticles using high-resolution cryo-TEM. *Microsc Microanal*. 2006;12(2):145–150.
26. Wang YQ, Liang WS, Geng CY. Coalescence behavior of gold nanoparticles. *Nanoscale Res Lett*. 2009;4(7):684–688.
27. Dykman LA, Khlebtsov NG. Gold nanoparticles in biology and medicine: recent advances and prospects. *Acta Nat*. 2011;3(2):34–55.
28. Abraham GE, Himmel PB. Management of rheumatoid arthritis: rationale for the use of colloidal metallic gold. *J Nutr Med*. 1997;7:295–305.
29. Amer OS, Dkhil MA, Al-Quraishy S. Antischistosomal and hepatoprotective activity of *Morus alba* leaves extract. *Pak J Zool*. 2013;45(2):387–393.
30. Tousson E, Beltagy DM, Gazia MA, Al-Behbehani B. Expressions of P53 and CD68 in mouse liver with *Schistosoma mansoni* infection and the protective role of silymarin. *Toxicol Ind Health*. 2013;29(8):761–770.
31. El-Banhawey M, Ashry MA, El-Ansary AK, Aly SA. Effect of *Curcuma longa* or parziquantel on *Schistosoma mansoni* infected mice liver – histological and histochemical study. *Indian J Exp Biol*. 2007;45:877–889.
32. Dkhil MA, Bauomy AA, Diab MSM, Wahab R, Delic D, Al-Quraishy S. Impact of gold nanoparticles on brain of mice infected with Schistosoma mansoni. *Parasitol Res*. 2015;114(10):3711–3719.
33. Cunha GM, Silva VM, Bessa KD, et al. Levels of oxidative stress markers: correlation with hepatic function and worm burden patients with schistosomiasis. *Acta Parasitol*. 2012;57:160–166.
34. Bauomy AA, Diab MSM, Abdel Moneim AE, Dkhil MA, Al-Quraishy S. Neuronal activities of berberine in *Schistosoma mansoni*-infected mice. *Afr J Pharm Pharmacol*. 2013;7(7):368–374.
35. Moukoko CE, El Wali N, Saeed OK, et al. No evidence for a major effect of tumor necrosis factor alpha gene polymorphisms in periportal fibrosis caused by *Schistosoma mansoni* infection. *Infect Immun*. 2003;71(10):5456–5460.
36. Voronov E, Dotan S, Gayvoronsky L, et al. IL-1-induced inflammation promotes development of leishmaniasis in susceptible BALB/c mice. *Int Immunol*. 2010;22(4):245–257.
37. Zhang Y, Chen L, Gao W, et al. IL-17 neutralization significantly ameliorates hepatic granulomatous inflammation and liver damage in *Schistosoma japonicum* infected mice. *Eur J Immunol*. 2012;42(6):1523–1535.
38. Abdallahi OM, Bensalem H, Diagana M, De Reggi M, Gharib B. Inhibition of nitric oxide synthase activity reduces liver injury in murine schistosomiasis. *Parasitology*. 2001;122(Pt 3):309–315.
39. Ding AH, Nathan CF, Stuehr DJ. Release of reactive nitrogen intermediates and reactive oxygen intermediates from mouse peritoneal macrophages. Comparison of activating cytokines and evidence for independent production. *J Immunol*. 1988;141(7):2407–2412.
40. Mwatha JK, Kimani G, Kamau T, et al. High levels of TNF, soluble TNF receptors, soluble ICAM-1, and IFN-gamma, but low levels of IL-5, are associated with hepatosplenic disease in human *Schistosomiasis mansoni*. *J Immunol*. 1998;160(4):1992–1999.
41. Khan HA, Abdelhalim MA, Alhomida AS, Al-Ayed MS. Effects of naked gold nanoparticles on proinflammatory cytokines mRNA expression in rat liver and kidney. *Biomed Res Int*. 2013;2013:2–6.
42. Shukla R, Bansal V, Chaudhary M, Basu A, Bhonde RR, Sastry M. Biocompatibility of gold nanoparticles and their endocytotic fate inside the cellular compartment: a microscopic overview. *Langmuir*. 2005;21(23):10644–10654.

43. Zhang Q, Hitchins VM, Schrand AM, Hussain SM, Goering PL. Uptake of gold nanoparticles in murine macrophage cells without cytotoxicity or production of pro-inflammatory mediators. *Nanotoxicology*. 2011;5:284–295.
44. Tournebize J, Boudier A, Joubert O, et al. Impact of gold nanoparticle coating on redox homeostasis. *Int J Pharm*. 2012;438:107–116.
45. Ishak K, Baptista A, Bianchi L, et al. Histological grading and staging of chronic hepatitis. *J Hepatol*. 1995;22(6):696–699.

International Journal of Nanomedicine

Dovepress

Publish your work in this journal

The International Journal of Nanomedicine is an international, peer-reviewed journal focusing on the application of nanotechnology in diagnostics, therapeutics, and drug delivery systems throughout the biomedical field. This journal is indexed on PubMed Central, MedLine, CAS, SciSearch®, Current Contents®/Clinical Medicine, Journal Citation Reports/Science Edition, EMBase, Scopus and the Elsevier Bibliographic databases. The manuscript management system is completely online and includes a very quick and fair peer-review system, which is all easy to use. Visit http://www.dovepress.com/testimonials.php to read real quotes from published authors.

Submit your manuscript here: http://www.dovepress.com/international-journal-of-nanomedicine-journal